Interaction of CO and NO with PdCu(111) Surfaces

F. Illas* and N. López

Departament de Química Física, Facultat de Química, Universitat de Barcelona, C/Martí i Franquès 1, 08028-Barcelona, Spain

J. M. Ricart and A. Clotet

Departament de Química Física i Inorgànica, Facultat de Química, Universitat Rovira i Virgili, Pl. Imperial Tarraco, 43005-Tarragona, Spain

J. C. Conesa and M. Fernández-García

Instituto de Catálisis y Petroleoquímica, CSIC, Campus Cantoblanco, 28049 Madrid, Spain

Received: May 5, 1998; In Final Form: July 20, 1998

A theoretical study of the structural parameters, interaction energies, and bonding mechanism of CO and NO to a Pd center located in two copper-rich bimetallic PdCu(111) surfaces and several coordination positions of the Pd(111) surface is reported. For CO, the bonding nature is predominantly covalent, and the analysis of bonding nature variations through the series is used to interpret the experimentally observed decrease of the CO/PdCu interaction energy with the increase in copper percentage of the alloy, the insensitivity of the C−O stretch frequency to the composition of the central Pd environment, and the linear correlation observed between the CO desorption energy and the X-ray photoelectron spectroscopy (XPS) core-level shift. For NO, the nature of the interaction varies from nearly covalent for pure Pd to a mixture of covalent plus ionic for copper-rich alloys; this parallels the expected growth of the ionic component of the bond with the decrease of the work function in going from Pd to Cu. A correlation between the N−O stretch frequency shift and the copper content of the binary systems is also found.

I. Introduction

The chemisorption of carbon monoxide and nitric oxide on metal surfaces has become a subject of great interest as part of the necessary activation steps during the catalytic reduction/oxidation of these molecules in industrial processes.[1] The adsorption of simple molecules, such as CO or NO, has also gained interest in being probe tests commonly used to obtain information concerning the chemical state of surfaces.[2,3]

PdCu systems have received attention in connection with its use in CO oxidation[4−6] and hydrogenation[7−10] and NO reduction[11] processes. The Pd−Cu binary system shows the existence of ordered phases and substitutional disordered fcc alloys.[12] Likewise, bcc disordered alloys have been also observed in the limited, 36−45, palladium atomic percent range.[12] Among these phases, the preparation methods used in catalysis, which make use of short calcination and/or reduction treatments, favor the appearance of disordered fcc alloy close-packed particles. These binary particles do not present significant copper segregation to the surface.[13,14] Consequently, disordered binary fcc phases constitute the subject of the majority of the studies performed in such bimetallic systems.[1] In these PdCu phases, the surface Pd centers are negatively charged; the neighboring presence of copper moderately depopulates the Pd 4d subband mainly by inducing an internal hybridization of Pd which is larger than that corresponding to pure Pd metal and injects charge in the Pd 5sp subband. All these charge-transfer phenomena grow with the copper content of the alloy.[15] Interestingly, Pd centers in molecular PdCu dimers, that is, Pd centers with very small coordination numbers, are positively charged.[16] This contrasting fact is based on the huge difference in Pd−Cu coordination distances between the dimers and extended phases, which in the case of the dimer induces a larger involvement of the Pd 4d level in the heterometallic bond, allowing a larger Pd loss of charge and, hence, the existence of positively charged Pd.[15]

The CO and NO adsorption over PdCu alloys have been extensively studied in recent years. Heats of adsorption of these molecules on Pd surface centers of the bimetallic phase are weaker than on pure, single metals.[1,16−17] The differential adsorption energetics has been attributed to a direct effect of the metal d subband contribution to the CO/substrate interaction.[18] However, PdCu alloys exhibit valence bands quite different from those of pure Pd. Therefore, in addition to (possible) changes in the chemical or charge-transfer components of the CO/surface bond, other bonding components related to the Pauli repulsion should be expected.[15] In contrast to the energy behavior, the C−O and (to a lesser extent) the N−O stretch frequencies are rather insensitive to the presence of copper in the surroundings of Pd.[1,9,14] For CO there is another interesting experimental result arising from photoemission studies. Rodriguez and Goodman were the first to show the existence of a strong correlation between core-level shifts and CO desorption temperature, this correlation appearing in an important number of bimetallic overlayer systems.[19] This was later rationalized on the basis of the above-mentioned primacy of the d metal−$2\pi^*$ CO interaction; it implies that the interaction energy is primarily governed by the 4d Pd subband energy position,[18] which should shift in the same direction (to higher binding energy) as core levels,[15] thus establishing a correlation between both magnitudes.

S1089-5647(98)02118-X CCC: $15.00
Published on Web 09/22/1998

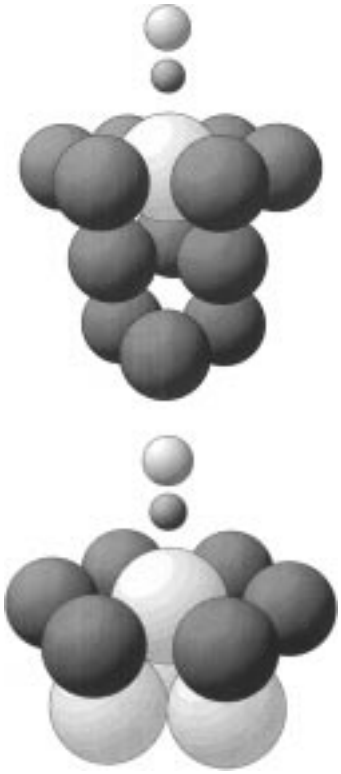

Figure 1. Schematic representation of CO and NO adsorption on a superficial Pd center of the Pd_1Cu_{12} (a, top) and Pd_4Cu_6 (b, bottom) clusters used to model PdCu alloys. Smaller spheres, Cu atoms; larger spheres, Pd atoms.

In an attempt to interpret the experimental results outlined above and further discuss previous theoretical analyses, we here report a theoretical ab initio cluster model study of the CO and NO/PdCu(111) systems. Two representative, Cu-rich surfaces of Pd_8Cu_{92} and $Pd_{40}Cu_{60}$ formal compositions will be studied. Particular attention will be paid to the CO interaction with these surfaces as this molecule is by far the most used in probe tests, and consequently, the corresponding experimental information is quite complete. A description of the theoretical background of the present approach is given in section II. This includes the key features and approximations of the cluster model and the analysis methods used to extract information from the wave functions. In section III we will compare the theoretical results with available experimental information, followed by the analysis of the adsorbate/surface interaction by using the constrained space orbital variation (CSOV)[20−22] method to decompose the energy into physically interpretable contributions and by an orbital projection technique[23,24] to obtain an estimation of the charge-transfer process between the adsorbate and the surface. The focus of our cluster model study is on the local features of the interaction between adsorbed molecules and PdCu surfaces—in particular, the trends that allow to interpret the experimental results from a rigorous physical basis using a theoretical approach that does not contain parameters fitted to experiment or make use of "a priori" assumptions on the importance of different terms in the electronic Hamiltonian. The aim of the present study is to analyze trends and to provide a qualitative understanding of the adsorbate−surface bond in these bimetallic systems.

II. Computational Details

A. Cluster Models and Theoretical Approach. The ab initio cluster model approach used here involves first the choice

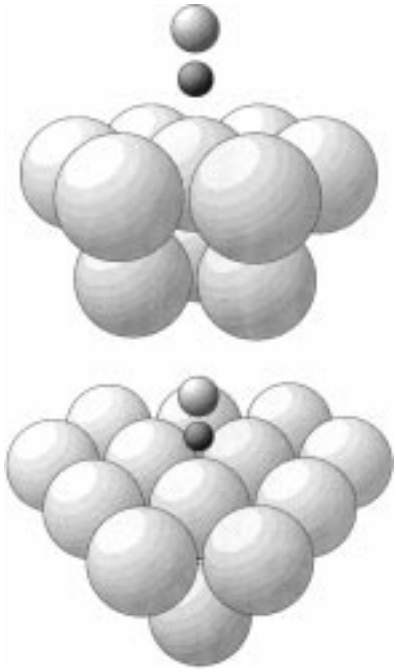

Figure 2. Schematic representation of CO and NO adsorption on the Pd_{10} (a, top) and Pd_{18} (b, bottom) clusters used to model the monocoordinated and three-coordinated positions, respectively, of the Pd(111) surface.

of a moderately large, albeit finite, cluster to represent the (111) surface of two PdCu alloys. This approach is particularly well suited because the disordered character of the binary fcc PdCu phases prevents the use of a periodic approach unless an extremely large unit cell is chosen. The second feature of the present approach is the use of purely ab initio methods of quantum chemistry which are used to variationally determine electronic wave functions or one-electron, Kohn−Sham, densities through the well-known ab initio Hartree−Fock (HF) or density functional theory (DFT) based quantum chemical methods. Further, the interaction of CO and NO with these surface model clusters is analyzed at the same level of theory.

The Pd_1Cu_{12} and Pd_4Cu_6 cluster models have been chosen to represent the (111) surfaces of PdCu substitutional disordered fcc alloys with Pd_8Cu_{92} and $Pd_{40}Cu_{60}$ formal composition. The first model contains three layers with seven atoms in the first layer, one Pd plus six Cu atoms, three in the second, and three in the third and intends to represent an essentially isolated surface Pd atom in a Cu matrix. As usual, this information can be abbreviated as $Pd_1(1,0,0)Cu_{12}(6,3,3)$. Similarly the second model, chosen to represent approximately a 50/50 alloy, is made up of two layers of metal atoms, and its composition is given by $Pd_4(1,3)Cu_6(6,0)$. These Pd_1Cu_{12} and Pd_4Cu_6 clusters are schematically shown in Figure 1. Atom−atom distances of 2.58 and 2.63 Å were employed for the Pd_1Cu_{12} and Pd_4Cu_6 clusters, respectively. These distances correspond to the average value in Pd_8Cu_{92} and $Pd_{40}Cu_{60}$ alloys; further details of these clusters can be found in ref 15.

The $Pd_{10}(7,3)$ and $Pd_{18}(12,6)$ cluster models (Figure 2) are also included in the calculations to represent monocoordinated and three-coordinated Pd centers of the (111) surface of the pure metal. The first one is used as a reference for comparison with bimetallic results while the second will be use to simulate the experimentally observed 3-fold adsorption site of CO at low coverages.[25] For NO, there is not complete confidence in the adsorption site assignment, but also the 3-fold coordination

seems to be the most likely candidate.[26] A Pd−Pd distance of 2.75 Å, corresponding to the bulk phase, is used for both Pd clusters.[15]

The NO and CO adsorption geometry on top of the Pd central atom of the bimetallic and Pd_{10} clusters and of the 3-fold position of Pd_{18} were found by direct energy minimization. The cluster atoms were kept frozen at their fcc bulk positions whereas the surface−adsorbate (S−A) distance perpendicular to the surface and the CO and NO internal equilibrium distances were optimized using analytical gradients of the energy. The dependence of the total energy with respect to the tilt angle was studied by performing suitable scans of the potential energy surface. These sections of the potential energy surface show a clear preference for the vertical orientation as expected. Consequently, the adsorbed molecules were kept perpendicular to the surface during the optimization of the distances described above. For both molecules, vibrational frequencies of the C−O, N−O, and S−A stretch modes have been calculated from the minima geometries using a normal-coordinate approach that consists of either moving the center of mass of the molecule in its fixed geometry or the adsorbed molecule internal distance while keeping the center of mass fixed at its equilibrium position above the surface.

For CO interacting with the different surface cluster models, restricted closed-shell Hartree−Fock (HF) or DFT calculations using the hybrid B3LYP scheme,[27] which includes the three-parameter Becke's exchange and Lee, Yang, and Parr correlation functionals, both based on the generalized gradient approach, have been performed. The interaction of NO with the cluster models, the result of an unrestricted open-shell calculation (UHF), has been chosen as a starting point for the correlated unrestricted B3LYP calculations. However, the UHF yields inconsistent results, mainly because of the very large spin contamination on the UHF determinant. Accordingly, only the unrestricted B3LYP (UB3LYP) ones are reported throughout this work.

The computations necessary to achieve a reasonable description of the bonding interaction in the present systems have been carried out by means of the HONDO[28] and Gaussian-94[29] computer codes. The molecular orbitals of the Hartree−Fock or Kohn−Sham determinants were expanded in basis sets of contracted Gaussian functions (CGTO's). For Pd atoms, the relativistic effective core potentials (RECP) reported by Hay and Wadt[30] have been used to describe the 1s−3d core while the electrons arising for the $4s^2$, $4p^6$, and $4d^{10}$ shells are treated explicitly (18-e RECP). Two GTO's basis sets have been used, both starting from the uncontracted 5s, 5p, and 4d primitive set reported by Hay and Wadt.[30] The first one uses a nonsegmented contraction scheme in which one s and one p primitive GTO are repeated, thus leading to a final [7s,7p,5d/3s,3p,2d] basis. The second basis is the internal LANL2DZ basis set included in Gaussian-94. For Cu atoms, the 1s−2p core is included in the RECP while the 3s, 3p, 3d, 4s, and 4p shells are explicitly described by means of GTO basis sets similar to those described for Pd. Since both contractions of the primitive sets led virtually to the same results, only the LANL2 results will be reported in the tables to avoid unnecessary duplication of information. For the N, C, and O atoms of the adsorbed CO and NO molecules, the standard 6-31G* basis set was used.[31]

B. Analysis of Wave Functions. To provide insights about the nature of the bonding of CO and NO to PdCu systems, we will make use of several theoretical methods of analysis. First, with the help of CSOV analysis[20−22] we decompose a given observable such as energy or dipole moment, calculated at HF level, into contributions arising from intraunit polarization (i.e., hybridization) and interunit charge transfer and covalent bonding effects.

In the CSOV analysis, the interaction between two fragments or units A and B is analyzed by computing HF wave functions where variational changes from the initial separated fragments are allowed to occur in well-defined, controlled steps. Each step measures a physically interpretable contribution to the studied observable in such a way that it is decomposed into a nonbonding contribution (Pauli or steric repulsion) plus bonding contributions corresponding to internal (intraunit) rehybridization or polarization and (interunit) charge-transfer contributions. In this process, step number 0 corresponds to the simple superposition of the separated frozen densities (FO = frozen orbital) of both fragments; the difference between results at this stage and the simple sum of values from the fragments measures the extent of the Pauli repulsion between them. Here it is worth mentioning that Pauli repulsion is a mean field property expected to be well reproduced at the HF level of theory. In fact, an estimate of the Pauli repulsion has also been obtained here at the B3LYP level; both HF and B3LYP values are found to be very similar in general terms. In the next step, the fragment A electron density is fixed, but the orbitals arising from fragment B are allowed to vary in their own basis space (which of course must be kept orthogonal to that of A), yielding the B polarization contribution to the observable. In CSOV step 2, the A orbitals are still fixed, but now the B orbitals are varied in a space that includes the virtual unoccupied molecular orbitals of A. This measures the effect of B to A charge transfer and covalent bonding, and unfortunately, it also accounts for a possible basis set superposition error (BSSE). However, as will be shown, the basis sets used are sufficiently large to avoid the occurrence of significant BSSE contributions. In a similar way, in CSOV step 3, the A orbitals are varied in its virtual space (while the occupied space of B is that obtained at step 2 and the virtual space of B is restored at its initial configuration and the whole set is properly orthogonalized), giving the A polarization contribution. Finally, in CSOV step 4, the A to B charge donation contribution is measured. The difference between the sum of all these contributions and the full variational, unconstrained result yields an estimation of the completeness of the variational freedom allowed to the wave function during the CSOV procedure, so that small values of this difference indicate that essentially all important bonding effects have been taken into account during the CSOV analysis.

In our case, we define the adsorbate, CO in this case, and the PdCu bimetallic clusters to be the two units A and B involved in the CSOV procedure; this allows to interpret intraunit polarization and interunit charge transfer as effects of CO to the bimetallic clusters or vice versa, giving physical basis to the interpretation of values obtained for the observables. The interaction energy, E_{int}, is then defined as

$$E_{int}(\text{CSOV; step } n) = E(\text{CO}) + E(\text{Pd}_x\text{Cu}_y) - E(\text{CO/Pd}_x\text{Cu}_y\text{; CSOV step } n) \quad (1)$$

The sign is such that a positive E_{int} indicates a net bonding interaction. The change in E_{int} between CSOV step n and the preceding step $n-1$, ΔE_{int}, represents the energetic importance of the new variational freedom allowed at step n. It should be noted that the $E(\text{CO/Pd}_x\text{Cu}_y\text{; CSOV step } n)$ term of (1) is not always a direct result of a simple calculation; details about the CSOV procedure can be found in refs 20−22. As indicated above, the FO contribution will be also analyzed for the DFT-

B3LYP wave functions in order to compare the electronic densities obtained with both methods of calculation. For completeness, the contribution, due to electronic correlation effects, which are implicitly included in the DFT calculations, will be attached to CSOV results. This correlation contribution is usually obtained from the difference between the HF and correlated energies. In this case the correlated energy is obtained from an hybrid, B3LYP, DFT result rather than from a correlated wave function based method. This is possible because Hartree−Fock is a well-defined approximation and B3LYP accounts for electronic correlation through the exchange-correlation functional.

The second method to characterize the bonding nature makes use of an orbital projection operator.[23,24] The projection of an orbital, $P(|\varphi\rangle)$, is the expectation value of the $|\varphi\rangle\langle\varphi|$ operator over the wave function of the system

$$P(|\varphi\rangle) = \langle\Psi|\varphi\rangle\langle\varphi|\Psi\rangle \qquad (2)$$

and measures the extent to which an orbital $|\varphi\rangle$ is contained in the total $|\Psi\rangle$ wave function. By comparing this value with that corresponding to an isolated fragment of the system, a measure of the extent of charge transfer between CO, NO, and PdCu alloys can be obtained. When fractional values, between 0 and 2 for a closed-shell system, are obtained, a correction for overlap of the bare fragments must be performed.[24] It should be noted that, as long as the adsorbate maintains its identity in the system, this measure of the orbital charge occupation does not include any arbitrary partition of the charge density as in Mulliken or related charge partitioning schemes and is much less basis dependent.[23,24] This method of charge measurement can yield a similar amount of information to that obtained from charge density plots. The main problem associated with these two last methods is the partial coupling of charge polarization effects with charge-transfer processes that, in this case, are uncoupled (vide supra) by using this method in conjunction with the CSOV technique presented in this section. The projection study will be performed on the Kohn−Sham orbitals obtained from the B3LYP calculation. As recently shown by Baerends et al.,[32] Kohn−Sham potentials used in DFT calculations build a correct electronic density and, therefore, can be used to analyze charge transfer or displacement between adsorbate and surface with reasonable confidence. For NO, the use of an unrestricted formalism (UB3LYP) forces to separately project the α and β spin orbitals, although meaningful results correspond to the sum of both components.

III. Results and Discussion

A. Comparison with Experimental Results. The optimized geometrical parameters, S−A and C−O and N−O distances, and the energies of adsorption for the ground state of the present adsorbate−surface systems are reported in Table 1. For the NO/surface systems the expectation value of the square of the total spin operator, $\langle S^2\rangle$, is also included in the set of results presented in Table 1. The upright position of both molecules is in agreement with experimental reports.[25,26] For CO and independently of the level of theory, there is an increase of the S−A distance with the copper content of the alloy, this fact being more pronounced for the HF results. The only known experimental data are S−C distances of 1.27 ± 0.05[25] and 1.93 ± 0.07 Å[33] for adsorption of CO on Pd(111) at low (3-fold) at high (on-top) coverages, respectively, which compare reasonably well with the HF results for our CO/Pd_{18} and CO/Pd_{10} model systems. It is worth mentioning that the agreement between experimental and the B3LYP calculated results is even better and, surprisingly enough, is within the experiment error bars. The above results show that, as expected, structural parameters are local properties that are not largely affected by cluster size. This is also the case for core-level shifts and vibrational frequencies. For NO we report only UB3LYP results because the UHF method does not appear to be able to properly describe this adsorbate−substrate interaction (vide infra). The growth of the S−A distance also parallels the copper content of the bimetallic clusters. It is interesting to note that the NO/surface ground states have, in general, important spin contaminations, as has been reported previously for NO/Pd(110).[34] Note that for pure Pd we have also studied a high spin state with $S_z = 1.5$, which is almost degenerate with that reported in Table 1 (1.01 vs 1.07 eV) and does not show significant differences in the geometrical parameters.

TABLE 1: HF/DFT-(U)B3LYP Results for CO and NO Adsorption on PdCu and Pd Cluster Models; Equilibrium Distance from the Adsorbate to the Surface, d_{S-A}, and Equilibrium C−O and N−O Distances, d, in Å, and Interaction Energy, D_e, in eV[a]

	CO			NO			
model/method	d_{S-A}	d	D_e	d_{S-A}	d	D_e	$\langle S^2\rangle$
Pd_{18} HF	1.36	1.14	1.46				
Pd_{18} (U)B3LYP	1.29	1.19	1.64				
Pd_{10} HF	1.89	1.11	1.32				
Pd_{10} (U)B3LYP	1.93	1.15	1.05	1.90	1.16	1.07	4.65
Pd_4Cu_6 HF	2.19	1.12	0.08[b]				
Pd_4Cu_6 (U)B3LYP	1.97	1.15	1.27	1.97	1.18	0.51	0.76
Pd_1Cu_{12} HF	2.61	1.15	0.03[b]				
Pd_1Cu_{12} (U)B3LYP	2.06	1.15	0.75	2.35	1.17	0.91	1.89

[a] For NO, the expectation value of the S^2 operator for the ground state is also included in the table. [b] BSSE corrected values.

At the DFT, (U)B3LYP, level of theory the energetic behavior of both molecules, CO and NO, above the different surface cluster models agrees well with experimental trends observed.[1,3,17] Pd centers in bimetallic surfaces adsorb CO and NO less strongly than in single, homometallic surfaces, showing a tendency to weaker adsorption energies with the copper content of the alloy composition for CO and a more complex behavior for NO, decreasing for alloys close to 50/50 composition and almost maintaining the magnitude corresponding to pure Pd for (very) Cu-rich alloys. The decrease of 0.37 eV for CO adsorption on Pd_4Cu_6 with respect to Pd_{18} can be favorably compared with the experimental difference (0.15 eV) observed for adsorption on Pd(111) and $Pd_{50}Cu_{50}$(111) at low coverage.[1,17]

Other experimental observables often analyzed in the literature such as the vibrational C−O and N−O stretch frequencies[1,3,8] have been calculated and included in Table 2. The C−O stretch shows the already mentioned insensitivity to the homo- or heterocomposition of the Pd environment while the N−O one seems to present a moderate red shift paralleling the copper content of the system. Note, however, that the N−O stretch in pure Pd systems is not very sensitive to coordination number,[34] showing, as will be discussed later, that the presence of Cu induces changes in the chemical components of the NO−Pd interaction and has consequences in the adsorbate/surface bond. With respect to CO, very similar results observed at HF and B3LYP levels show that inclusion of correlation only induces a lowering of the potential energy surface (PES) without significantly changing its shape. This may be attributed to the fact that the main electronic correlation effect is on the total energy. In Table 2, the S−CO and NO stretch frequencies are also reported. Both series, CO and NO, show the effect of the coordination distance increase with copper content.

TABLE 2: Vibrational Frequencies Corresponding to the Frustrated Surface to Adsorbate Translation, ν_s(S−A) and C−O (N−O) Stretching Mode, ν_s(C−O) (ν_s(N−O)), for the Equilibrium Geometries of Table 1[a]

	CO		NO	
model	ν_s(S−A)	$\Delta\nu_s$(C−O)	ν_s(S−A)	$\Delta\nu_s$(N−O)
Pd_{10} HF		−28		
Pd_{10} (U)B3LYP	343	−36	339	−146
Pd_4Cu_6 HF		−102		
Pd_4Cu_6 (U)B3LYP	331	−56	207	−202
Pd_1Cu_{12} HF		−40		
Pd_1Cu_{12} (U)B3LYP	256	−30	112	−250

[a] All results in cm^{-1}. ν_s(C−O) and ν_s(N−O) are expressed as shift, $\Delta\nu_s$(C−O) and $\Delta\nu_s$(N−O), with respect to the corresponding free molecule. HF $\nu_s(C-O)_{free} = 2442\ cm^{-1}$; DFT $\nu_s(C-O)_{free} = 2119\ cm^{-1}$; DFT $\nu_s(N-O)_{free} = 1895\ cm^{-1}$.

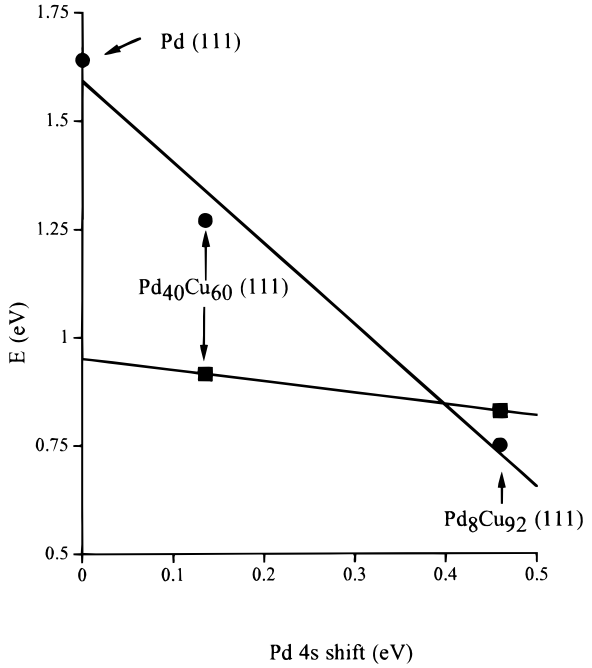

Figure 3. Correlation between Pd core-level shifts (eV) in PdCu alloys and CO adsorption energy (circles) or d(metal) to $2\pi^*$ CO interaction energy (squares) as obtained from the CSOV calculations, in eV. Results are BSSE corrected. See text for details.

Next, we analyze the relationship between E_{int} and core-level shifts in the Pd surface centers. Figure 3 shows the descending linear correlation existent between core-level shift in Pd surface centers and the B3LYP CO adsorption energy, in accordance with the general trend already observed by Rodriguez and Goodman.[19] DFT values are used instead of HF ones as they give a better representation because of the inclusion of correlation effects on the final electronic density.[32] The inclusion of electronic correlation permits to adequately describe the interaction energy and modestly reduces the oscillation with cluster size of the interaction energies. The origin of these oscillations has been found to lie in the limited representation of the surface conduction band by clusters, and it is already observed in the frozen orbital contribution to the interaction energy.[32,35] Notice that the value of E_{int} for CO on Pd_4Cu_6 is slightly larger than the one corresponding to Pd_{10}; this may reflect a cluster size dependence. However, Figure 3 shows that despite a possible dependence of E_{int} with respect to cluster size (not larger than ≈0.25 eV), the present cluster models qualitatively reproduce the experimental trend. In Figure 3, the Pd 4s shifts with respect to the Fermi edge of the system (taken from ref 15) have been used instead of the $3d_{5/2}$ Pd ones, which is the most broadly reported in XPS studies.[1,3] Calculations on the $3d_{5/2}$ level are not possible because these core electrons are included in the RECP operator.[15] For systems in which the photoemission phenomenon is dominated by the initial state contribution, as occurs here,[15] all electronic levels should shift in the same direction (to higher binding energy), although the more shallow nature of the 4s level, with respect to the $3d_{5/2}$ one, will tend to reduce the magnitude of the shift by about 30%.[15] In any case, the experimental observations made with the $3d_{5/2}$ Pd levels are also valid for the 4s one, as can immediately be deduced from Figure 3.

TABLE 3: CSOV Analysis for the HF Interaction Energy ($E_{int}/\Delta E_{int}$, eV) between CO and Mono- and Bimetallic Clusters for a Fixed Geometry ($d_{S-A} = 2.00$ Å, $d_{C-O} = 1.15$ Å)[a]

CSOV step	CO/Pd_{10}	CO/Pd_4Cu_6	CO/Pd_1Cu_{12}
0.F.O.	−2.339 (−2.03)	−2.563 (−2.04)	−2.766 (−2.41)
1.Pol. Cluster	−0.591/1.748	−1.657/0.906	−1.882/0.884
2.Don. Cluster	−0.003/0.594	−0.689/0.968	−0.979/0.903
3.Pol. CO	0.167/0.164	−0.582/0.107	−0.863/0.116
4.Don. CO	1.038/0.871	0.047/0.629	−0.229/0.634
5.SCF	1.238/0.200	0.152/0.105	−0.118/0.111
6.E_{corr}		1.265/1.113	0.730/0.848

[a] B3LYP results for the F.O. contribution are given in parentheses; E_{corr} stands for the electronic correlation contribution to $E_{int}/\Delta E_{int}$.

B. Bonding Nature. Consequences of the Observables. As discussed in the previous section, there is a general agreement between the values calculated for the observables with local character and the experimentally reported values. Therefore, we will focus this subsection in the analysis of the bonding nature of the CO and (in lesser extent) NO interaction with Pd surface centers of the monometallic reference and bimetallic clusters. This will permit to qualitatively interpret the trends described for the energetic and vibrational observables.

A CSOV analysis of the CO/surface interaction for the CO/Pd_{10}, CO/Pd_4Cu_6, and CO/Pd_1Cu_{12} systems at a fixed geometry ($d_{S-A} = 2.00$ Å, $d_{C-O} = 1.15$ Å) is reported in Table 3. This geometry is chosen close to the B3LYP equilibrium one (Table 1) and is fixed for all systems in order to allow an easier interpretation of the trends. The FO contribution grows with copper content; this is an expected result since the local occupation of sp levels of Pd centers also increases with copper content.[15] Note, however, that the increase is only of moderate magnitude (20%) for both HF and B3LYP levels of theory. In accordance, the equilibrium geometries present a smooth increase of the Pd−C distance with the copper content of the alloy. More interesting is the fact that the charge-transfer or chemical contributions (donations) do not show large differences between different alloy systems although there is a rather significant difference between pure Pd and the alloys. The presence of copper, with respect to Pd, increases the metal $d_\pi \rightarrow$ CO ($2\pi^*$) contribution by about 30% (see don. cluster in Table 3) and reduces the CO (5σ) → metal dsp one by ≈30% (don. CO in Table 3), but both components do not show any significative trend with alloy composition—this despite the different d/sp electronic occupation presented for Pd surface centers in these clusters.[15] Hence, these results suggest that the donation contribution is more affected by the change of the Fermi level nature (which is mainly of Cu 4sp nature for Cu-rich alloys and Pd 4d5sp for Pd) than by its degree of occupancy. On the other hand, the back-donation is dominated by the energy shift to higher binding energies observed for 4d Pd-like levels in Cu-rich alloys, and again, the (moderate) variation in occupancy of these levels is of secondary importance. The HF

TABLE 4: Expectation Values (Increment of Electrons) of the 5σ and 2π* Orbitals of CO Adsorbed on Mono- and Bimetallic Clusters

	CO	
model	5σ	2π*
Pd_{10}	−0.09	0.46
Pd_4Cu_6	−0.08	0.52
Pd_1Cu_{12}	−0.07	0.49

energy is almost recovered by the cluster polarization; minor contributions from CO polarization and the coupling among modes (the SCF contribution) are observed. In essence, the CSOV analysis shows a very similar covalent bonding among these systems with the typical CO(5σ) donation and the back-donation to CO(2π*) contributions. The energetic description of CO/surface systems is then completed by adding the equally important cluster polarization and correlation contributions. Here, it is necessary to stress that correlation contributions are defined, as usual, as the energy difference between Hartree−Fock and correlated energies. In the present case the correlated calculation is chosen to be the B3LYP which includes correlation through the exchange-correlation functional.

From the above CSOV analysis we first notice that the energy difference between the FO step an the unconstrained HF is quite large, ≈3.5 eV, but in many cases it is not enough to account for the observed interaction energies; the reason for this failure of the HF is the lack of electronic correlation effects which usually make a large net contribution to the bond.[35b,36−38] This contribution is implicitly included in the exchange-correlation part of the B3LYP functional. This is the reason why the B3LYP energies are in agreement, even quantitatively, with experiment. It is worth pointing out that the HF Pauli repulsion is always 0.3−0.5 eV larger than the DFT, B3LYP, one. At first sight, this fact may appear to be somehow surprising because one would expect that HF would be able to accurately describe such a mean field quantity. However, we must recall that the densities which are superimposed are either the HF or B3LYP, and they must be different.[32] Hence, the correlation contribution presented in Table 3 includes an overestimation of the FO measured at the HF level that can be eliminated by using the corresponding values obtained with the B3LYP functional. Under this premise, we have additional net bonding contributions of 0.78 and 0.49 eV for the CO/Pd_4Cu_6 and CO/Pd_1Cu_{12} systems, respectively, that are due to electronic correlation effects. On the other hand, it can be noted that, except for the cluster polarization, the remaining HF contributions to the interaction energy can be taken as accurate enough. This is shown by the similar picture emerged from both formalisms for the chemical or charge-transfer contributions (results are given in Table 4) as well as the similarity in the PES surface shapes deduced from the C−O and N−O stretch frequencies. The limited description of the cluster polarization is obviously a drawback implicit in the cluster representation of the surface, whose consequences are limited here by using clusters of similar size and studying the trends of the observables and not their absolute magnitudes.

The above analysis of the bonding of CO to pure Pd and PdCu alloy surfaces is further confirmed with the analysis of the charge transfer which, we would like to remark, is done on the Kohn−Sham orbitals derived from B3LYP calculations. The projection of the 5σ and 2π* CO orbitals shows a constant change of charge of -0.08 ± 0.01 and $+0.49 \pm 0.03$ electrons, respectively, along the series. These figures are very similar to those reported for the bridge CO adsorption on Pd(100),[39] further supporting the small surface sensitivity of the chemical or charge-transfer components of the adsorption process. Note, however, that for small cluster (dimers) the picture is again different; alloying in the PdCu dimer is claimed to reduce the back-donation capability of the Pd atom to CO relative to Pd_2, in accordance with the significant loss of charge observed for these center dimers.[16]

The key point to extract from the CSOV analysis is that the CO/surface bonding is not solely dominated by a single contribution. This is in opposition to results presented in ref 18 for a more extended series of alloys and bimetallic overlayers. On the other hand, the descending trend observed for the interaction energy with copper content in PdCu systems seems to be mainly associated with variations in the Pauli repulsion and, more importantly, in electronic correlation contributions. So, the linear dependence experimentally observed between the interaction energy and the core-level shifts of the isolated alloys should be mainly grounded in this last mentioned contribution. In fact, although the magnitude of the Pd 4s shift is dominated by the initial-state Pd polarization (hybridization) in response to the presence of copper, the correlation contribution to the shift has the larger variation between the bimetallic clusters studied; in going from Pd_4Cu_6 to Pd_1Cu_{12}, the differential polarization of the electronic clouds in response to the heterometallic bond formation has almost a null contribution due to a compensation effect between Pd and Cu; the differential charge transfer only produces a 0.12 eV increment of the 4s shift while the differential correlation contribution is responsible for a 0.22 eV increment.[15] The 0.12 plus 0.22 eV (total of 0.34 eV) accounts for the difference in the 4s shift between both systems (0.46 eV for Pd_1Cu_{12} versus 0.14 eV for Pd_4Cu_6). We must therefore stress that the BSSE corrected CO (2π*) back-donation contribution (squares in Figure 3) definitively does not explain the E_{int}/XPS shift linear relationship, as has been proposed for metal overlayers,[18] pointing out a different chemical interpretation of the phenomenon in alloys, at least PdCu alloys, and overlayers. This may be related to different strain consequences originating from variations in heteroatomic distances; as previously mentioned, for PdCu systems, charge transfer between heteroatoms seems to be strongly sensitive to this property, and the resulting drastic differences in the electronic configuration of surface Pd centers are likely to affect significantly the behavior upon adsorption. Finally, the CSOV (Table 3) and projection (Table 4) analyses explain the C−O stretch insensitivity to alloy composition: as charge-transfer processes and Pauli repulsion do not vary significantly with copper content, only the correlation contribution is expected to influence this observable, but its variation with the internal C−O coordinate is usually of low to moderate magnitude.[36]

For NO, the inconsistent UHF results do not allow to make a CSOV analysis of the bond. One may think that a better approach would have been a ROHF method. However, the interaction of NO with metal surfaces, at least Cu and Ag, involves a charge transfer with the formation of an ionic bond.[36] The proper description of such a process requires the use of more than a single Slater determinant, and in such a case, inclusion of dynamical correlation through DFT is not straightforward.[40,41] The failure of UHF is precisely related to this multideterminantal description; the UHF tries to mix the important configurations resulting in very large spin contaminations and absurd distances. The fact that more than one Slater determinant is needed may also be relevant for the DFT calculations. Therefore, we will omit further extensive analysis of the interaction of NO with metal surfaces. We would like just to mention that projection analyses of the charge-transfer

process based on the Kohn−Sham orbitals from B3LYP calculations indicate that the NO/surface bonding interaction is varying through the series. The decreasing work function of the systems with the copper content (our Pd_{10}, Pd_4Cu_6, and Pd_1Cu_{12} clusters yield work functions of 4.28, 3.65, and 3.51 eV, respectively, which parallel the descending behavior shown experimentally with the copper content)[15] is likely to explain the results. For Pd, the NO adsorption nature seems to be covalent, with a very modest charge transfer, as reported for other Pd surfaces.[34] We must advert that the study in ref 34 is also based in the use of a single Kohn−Sham determinant and may suffer the same above-described deficiencies. For the bimetallic systems, the dominant Cu 4sp nature of the Fermi region induces a decrease of the work function with respect to Pd(111) and favors the metal−$2\pi^*$ NO contribution, charging the adsorbed molecule in a similar way for both binary systems. The N−O stretch frequency red shift, however, seems to correlate with the copper content of the systems (Table 2), probably due to the reduction of the positive Pauli repulsion contribution originated by the growth of the coordination distance.

IV. Conclusions

We have reported a theoretical description of the nature and characteristics of the CO and NO adsorption on PdCu(111) alloy surfaces using several cluster models and ab initio HF wave functions and the B3LYP hybrid DFT approach. Our focus has been the study of the bonding nature of the CO and NO interaction with Pd and PdCu(111) surfaces and its influence in the energetic and vibrational observables.

For CO, it has been shown that the energy of interaction contains several contributions of equal magnitude without dominance of the $2\pi^*$ back-donation. In PdCu alloys the Pauli repulsion is overcome by the chemical 5σ donation and $2\pi^*$ back-donation, alloy polarization, and correlation contributions. The decreasing behavior of the interaction energy with copper content of the alloy and its linear behavior with core-levels shifts are mainly a consequence of the diminishing correlation contribution. The predominance of this contribution also enables to rationalize the C−O stretch insensitivity to alloy composition.

For NO, the bonding nature of the system changes through the series studied; the neighboring presence of Cu introduces a ionic contribution due to the reduction of the work function of the alloy with copper content. This implies that chemical or charge-transfer contributions to the interaction energy are expected to count and that the progressive red shift observed for the N−O stretch frequency may serve as a tool in probing the chemical composition of PdCu surfaces.

Acknowledgment. M.F.-G. thanks the Consejo Superior de Investigaciones Científicas (CSIC) for a Postdoctoral Contract. Financial support by CICyT (projects MAT94-0835-CO3-02 and PB95-0847-CO2-01 and PB95-0847-CO2-02), CAM (project 06 M/085/96), and NATO (CRG 941191) is fully acknowledged. The authors thank the Centre de Supercomputació de Catalunya (CESCA) for helping with part of the calculations.

References and Notes

(1) Niewnhuys, B. E. *Surf. Sci. Lett.* **1996**, *3*, 1869.
(2) Hollins, P. *Surf. Sci. Rep.* **1992**, *16*, 51.
(3) Rodriguez, J. A. *Surf. Sci. Rep.* **1996**, *24*, 223.
(4) Choi, K. I.; Vannice, M. A. *J. Catal.* **1991**, *131*, 36.
(5) Espeel, P. H.; De Peuter, G.; Trelen, M. C.; Jacobs, P. A. *J. Chem. Phys.* **1994**, *98*, 11588.
(6) Martínez-Arias, A. Private communication.
(7) Ponec, V.; Bond, C. G. *Catalysis by Metals and Alloys*; Elsevier: Amsterdam, 1995.
(8) Anderson, J. A.; Fernández-García, M.; Haller, G. L. *J. Catal.* **1996**, *164*, 477.
(9) Anderson, J. A.; López-Granados, M.; Fernández-García, M. *J. Catal.*, in press.
(10) Leon y Leon, C. A.; Vannice, M. A. *Appl. Catal.* **1991**, *69*, 305.
(11) Fernández-García, M. Unpublished results.
(12) Villards, A. P.; Calvet, L. D. *Pearson's Handbook of Crystallographic Data for Intermetallic Phases*; ASM Int.: Materials Park, OH, 1991.
(13) Fernández-García, M.; Márquez-Alvarez, C.; Haller, G. L. *J. Phys. Chem.* **1995**, *99*, 12565.
(14) Fernández-García, M.; Anderson, J. A.; Haller, G. L. *J. Phys. Chem.* **1996**, *100*, 16247.
(15) Fernández-García, M.; Conesa, J. C.; Clotet, A.; Ricart, J. M.; López, N.; Illas, F. *J. Phys. Chem. B* **1998**, *102*, 141.
(16) Rochefort, A.; Fournier, R. *J. Phys. Chem.* **1996**, *100*, 13506.
(17) Debauge, Y.; Abon, M.; Bertolini, J. C.; Massardier, J.; Rochefort, A. *Surf. Sci.* **1995**, *90*, 15.
(18) Hammer, B.; Morikawa, Y.; Norskov, J. K. *Phys. Rev. Lett.* **1996**, *76*, 2141.
(19) Rodriguez, J. A.; Goodman, D. W. *Science* **1992**, *257*, 897.
(20) Bagus, P. S.; Herman, K.; Bauschlicher, C. W. *J. Chem. Phys.* **1984**, *80*, 4378.
(21) Bagus, P. S.; Herman, K.; Bauschlicher, C. W. *J. Chem. Phys.* **1984**, *81*, 1966.
(22) Bagus, P. S.; Illas, F. *J. Chem. Phys.* **1992**, *96*, 8962.
(23) Pacchioni, G.; Illas, F.; Philpott, M. P.; Bagus, P. S. *J. Chem. Phys.* **1989**, *90*, 4287.
(24) Bagus, P. S.; Illas, F. *Phys. Rev. B* **1990**, *42*, 10852.
(25) Fernández, V.; Bradshaw, A. M.; Baddeley, C.; Lee, A. F.; Lambert, R. M.; Woodruff, D. P.; Fritzsche, V. *Z. Phys. Chem.* **1997**, *198*, 73.
(26) Ransier, R. D.; Gao, Q.; Waltenburg, H. N.; Lee, K.-W.; Nooij, O. W.; Lefferts, L.; Yates, J. T. *Surf. Sci.* **1994**, *320*, 209.
(27) Becke A. *Phys. Rev. A* **1988**, *38*, 3098. Lee, C.; Yang, W.; Parr, R. G. *Phys. Rev. B* **1988**, *37*, 785.
(28) Dupuis, M.; Johston, F.; Márquez, A. *HONDO 8.5 for CHEMstation*. IBM corporation, Neighborhood Road, Kingston, NY 12401. CSOV adaptation by F. Illas, J. Rubio, and A. Márquez.
(29) Frisch, M. J.; Trucks, G. W.; Schlegel, H. B.; Gill, P. M. W.; Johnson, B. G.; Robb, M. A.; Cheeseman, J. R.; Keith, T.; Petersson, G. A.; Montgomery, J. A.; Raghavachari, K.; Al-Laham, M. A.; Zakrzewski, V. G.; Ortiz, J. V.; Foresman, J. B.; Peng, C. Y.; Ayala, P. Y.; Chen, W.; Wong, M. W.; Andres, J. L.; Replogle, E. S.; Gomperts, R.; Martin, R. L.; Fox, D. J.; Binkley, J. S.; Defrees, D. J.; Baker, J.; Stewart, J. P.; Head-Gordon, M.; Gonzalez, C.; Pople J. A. *Gaussian 94, Revision B.3*; Gaussian, Inc.: Pittsburgh, PA, 1995.
(30) Hay, P. J.; Wadt, W. R. *J. Chem. Phys.* **1985**, *82*, 299.
(31) Hehre, W. J.; Radom, L.; Scleyer, P. R.; Pople, J. A. *Ab initio Molecular Orbital Theory*; Wiley: New York, 1985.
(32) Baerends, E. J.; Gritsenko, O. V. *J. Phys. Chem. A* **1997**, *101*, 5383.
(33) Behm, R. J.; Chirstmann, K.; Ertl, G.; Van Hove, M. A. *J. Chem. Phys.* **1980**, *73*, 2984.
(34) Pérez-Jigato, M.; Somasundram, K.; Termath, V.; Handy, N. C.; King, D. A. *Surf. Sci.* **1997**, *380*, 83.
(35) (a) Hermann, K.; Bagus, P. S.; Nelin, C. J. *Phys. Rev. Lett.* **1987**, *35*, 9467. (b) Bauschlicher, C. W., Jr. *J. Chem. Phys.* **1994**, *101*, 3250.
(36) Illas, F.; Ricart, J. M.; Fernández-García, M. *J. Chem. Phys.* **1996**, *104*, 5647.
(37) Illas, F.; Rubio, J.; Ricart, J. M.; Pacchioni, G. *J. Chem. Phys.* **1996**, *105*, 7192.
(38) Illas, F.; Ricart, J. M.; Clotet, A. *J. Phys. Chem. A* **1997**, *101*, 9732.
(39) Pacchioni, G.; Bagus, P. S. *J. Chem. Phys.* **1990**, *93*, 1209.
(40) Lieb, E. H. *Int. J. Quantum. Chem.* **1983**, *24*, 243.
(41) Moscardo, F.; San-Fabian, E. *Phys. Rev. A* **1991**, *44*, 1549. Moscardo, F.; Perez-Jimenez, A. J.; Sancho-Garcia; San Fabian, E. *Chem. Phys. Lett.*, in press.